

Original Article

γ -Secretase inhibitor DAPT sensitizes *t*-AUCB-induced apoptosis of human glioblastoma cells *in vitro* via blocking the p38 MAPK/MAPKAPK2/Hsp27 pathway

Jun-yang LI¹, Ru-jun LI², Han-dong WANG^{1, *}

¹Department of Neurosurgery, Jinling Hospital, School of Medicine, Nanjing University, Nanjing 210002, China; ²Department of Neurosurgery, Second Affiliated Hospital of Soochow University, Suzhou 215004, China

Aim: *Trans*-4-[4-(3-adamantan-1-yl-ureido)-cyclohexyloxy]-benzoic acid (*t*-AUCB) is a soluble epoxide hydrolase inhibitor that suppresses glioblastoma cell growth *in vitro*. The aim of this study was to examine whether the γ -secretase inhibitor *N*-[*N*-(3,5-difluorophenacetyl)-*l*-alanyl]-*S*-phenylglycine *t*-butyl ester (DAPT) could sensitize glioma cells to *t*-AUCB-induced apoptosis.

Methods: Both U251 and U87 human glioblastoma cell lines were tested. Cell growth was assessed using the cell counting kit-8. Cell apoptosis was detected with caspase-3 activity assay kits and flow cytometry. The protein levels in the p38 MAPK/MAPKAPK2/Hsp27 pathway in the cells were analyzed using Western blots.

Results: Pretreatment with DAPT (2 μ mol/L) substantially potentiated the growth inhibition caused by *t*-AUCB (200 μ mol/L) in U251 and U87 cells. Furthermore, pretreatment with DAPT markedly increased *t*-AUCB-induced apoptosis of U251 and U87 cells. *T*-AUCB alone did not significantly affect caspase-3 activity in the cells, but *t*-AUCB plus DAPT pretreatment caused significant increase of caspase-3 activity. Furthermore, pretreatment with DAPT completely blocked *t*-AUCB-induced phosphorylation of p38 MAPK, MAPKAPK2 and Hsp27 in the cells.

Conclusion: The γ -secretase inhibitor DAPT sensitizes *t*-AUCB-induced apoptosis of human glioblastoma cells *in vitro* via blocking the p38 MAPK/MAPKAPK2/Hsp27 pathway, suggesting that the combination of *t*-AUCB and DAPT may be a potentially effective strategy for the treatment of glioblastoma.

Keywords: glioma; chemotherapy; γ -secretase; DAPT; soluble epoxide hydrolase; *t*-AUCB; apoptosis; caspase-3; p38 MAPK; MAPKAPK2; Hsp27

Acta Pharmacologica Sinica (2014) 35: 825–831; doi: 10.1038/aps.2013.195; published online 5 May 2014

Introduction

Trans-4-[4-(3-adamantan-1-yl-ureido)-cyclohexyloxy]-benzoic acid (*t*-AUCB) is one of the improved soluble epoxide hydrolase (sEH) inhibitors. It has been well studied in cardiovascular and inflammatory diseases. Because of good oral bioavailability and improved pharmacokinetic properties, administering *t*-AUCB in drinking water has been recommended as a feasible, effective, and easy route of administration for chronic studies^[1]. One of our previous studies demonstrated that *t*-AUCB suppresses U251 and U87 cell growth by activating NF- κ B-p65 and induces cell-cycle G₀/G₁ phase arrest by regulating cyclin D1 mRNA and protein levels and CDC2 (Thr161)

phosphorylation^[2]. Then, another study revealed that *t*-AUCB elevates the activation of p38 MAPK, MAPKAPK2, and Hsp27 in U251 and U87 cells but does not induce cell apoptosis until the pre-treatment of the p38 MAPK inhibitor SB203580 or the Hsp27 phosphorylation inhibitor KRIBB3. This indicated that *t*-AUCB induces cell apoptosis after blocking a self-induced activation of Hsp27 and that the activation of Hsp27 may confer chemoresistance in glioblastoma cells^[3]. Thus, *t*-AUCB was considered to be a potential agent for glioma chemotherapy, and targeting the p38 MAPK/MAPKAPK2/Hsp27 pathway may be a new strategy for promoting the anti-tumor efficacy of *t*-AUCB.

Recently, γ -secretase inhibitors have gained increasingly more attention as a new anti-cancer drug because of their ability to block the Notch signaling pathway^[4,5]. The Lin research group showed that γ -secretase inhibitor-I at low concentra-

* To whom correspondence should be addressed.

E-mail njhdwang@hotmail.com

Received 2013-09-24 Accepted 2013-12-12

tions sensitized U87 and U251 cells to radiation by depleting radio-resistant CD133 cells^[5]. Therefore, to investigate whether γ -secretase inhibitor could sensitize glioma cells to *t*-AUCB treatment and overcome *t*-AUCB-induced apoptosis resistance, we chose *N*-[*N*-(3,5-difluorophenacetyl)-*l*-alanyl]-*S*-phenylglycine *t*-butyl ester (DAPT) for our study because it is widely applied in blocking the Notch signaling pathway. Our results showed that DAPT can indeed block the activation of the p38 MAPK/MAPKAPK2/Hsp27 pathway. DAPT strengthens *t*-AUCB-induced U251 and U87 cell growth suppression and sensitizes *t*-AUCB-induced apoptosis by blocking the activation of p38 MAPK/MAPKAPK2/Hsp27. Here we report our results showing that the γ -secretase inhibitor DAPT can target the p38 MAPK/MAPKAPK2/Hsp27 pathway and sensitize glioblastoma (GBM) cells to chemotherapy. We suggest that the combination of *t*-AUCB and DAPT is a potential strategy for the treatment of GBM.

Materials and methods

Agents

The sEH inhibitor *t*-AUCB was provided by Professor Bruce D HAMMOCK (Department of Entomology and UCD Cancer Research Center, University of California, Davis, CA, USA)^[1]. The γ -secretase inhibitor *N*-[*N*-(3,5-difluorophenacetyl)-*l*-alanyl]-*S*-phenylglycine *t*-butyl ester (DAPT) was purchased from Sigma-Aldrich (St Louis, MO, USA). In all assays, these agents were dissolved in dimethyl sulfoxide (DMSO) and subsequently diluted in serum-supplemented medium immediately before use. The DMSO concentration never exceeded 0.1% (*v/v*).

Cell culture

U251 and U87 human glioblastoma cell lines were purchased from the ATCC (American Type Culture Collection). All cells were maintained in DMEM (Dulbecco's modified Eagle's medium) containing 10% fetal bovine serum and 1% penicillin/streptomycin (complete medium). Cells were incubated at 37°C in a humidified atmosphere of 95% air and 5% CO₂.

Cell growth assay

Cell growth assays were performed using the Cell Counting Kit-8 (CCK-8) from Dojindo Laboratories (Kumamoto, Japan). As described in previous studies^[2], cells were plated onto a 96-well plate at a density of 5000 cells/well in 200 μ L of culture medium, and different experimental treatments were applied. Then, the cells were cultured in a humidified incubator containing 5% CO₂. After 48 h, 20 μ L of CCK-8 solution was added to each well and incubated for one hour. The optical density value (absorbance) was measured at 450 nm using an enzyme-linked immunosorbent assay plate reader (Bio-Rad Laboratories, Inc, Berkeley, CA, USA).

Caspase-3 activity assay

As we previously described^[3], the activity of caspase-3 in cells was measured using caspase-3 activity assay kits from Millipore (Kankakee, IL, USA). Absorbance was read at 405 nm in

a microtiter plate reader and represented the level of caspase-3 activity. Briefly, cell samples were collected, resuspended, and incubated in chilled 1 \times cell lysis buffer for 10 min and then centrifuged for 5 min at 4°C in a microcentrifuge (10000 \times g). The supernatants were then added to a 96-well plate and incubated for 1 h at 37°C in the working solution containing caspase-3 substrate, Ac-DEVD-pNA. The increase in caspase-3 activity was determined by comparing the absorbance from an apoptotic sample with an uninduced control after subtracting the background reading from cell lysates and buffers.

Apoptosis analysis by flow cytometry

For apoptosis analysis, cells were plated onto 10-cm culture dishes. Cells received different experimental treatments and were then collected by trypsinization, centrifuged (3500 r/min for 5 min), and washed twice with PBS. Cells were again collected and centrifuged, the supernatant was discarded, and the pellet was incubated for 15 min at room temperature with Annexin V-FITC and propidium iodide before analysis with a FACSaria III flow cytometer (BD Biosciences, San Jose, CA, USA).

Western blot analysis

As we previously described^[3], for the Western blot analysis, whole cell lysates were separated by SDS-PAGE and transferred to an Immobilon-P membrane (Millipore Corporation, Bedford, MA, USA). Membranes were probed with primary antibodies followed by incubation with secondary antibodies. Proteins were visualized with chemiluminescence luminol reagents (Beyotime Institute of Biotechnology, Shanghai, China). Antibodies against GAPDH (#2118), p38 MAPK (#9212), p-p38MAPK (Thr180/Tyr182) (#9215), MAPKAPK2 (#3042), p-MAPKAPK2 (Thr334) (#3041), Hsp27 (#2402), p-Hsp27 (Ser78) (#2405), and Notch1 intracellular region (#4147) were purchased from Cell Signaling Technology (Beverly, MA, USA). The densitometry of the immunoblotting bands was performed using ImageJ, a public software developed by the National Institutes of Health, USA.

Statistical analysis

Three experiments were performed for each assay. All data were analyzed by the Student-Newman-Keuls test and are expressed as the mean \pm standard deviation (SD). Difference with $P < 0.05$ were considered significant.

Results

DAPT strengthens *t*-AUCB-induced cell growth suppression

Our previous study demonstrated that *t*-AUCB inhibits U251 and U87 cell growth in a concentration-dependent manner and that 200 μ mol/L *t*-AUCB can cause significant cell growth suppression^[2]. In this study, U251 and U87 cells were treated for 48 h with DMSO (vehicle control), 2 μ mol/L DAPT only, 200 μ mol/L *t*-AUCB only, or 200 μ mol/L *t*-AUCB with a 4-h pre-treatment of 2 μ mol/L DAPT. Cell growth was detected using cell counting kit-8 (CCK-8) and quantified using the OD values (Figure 1). As the results show, *t*-AUCB alone

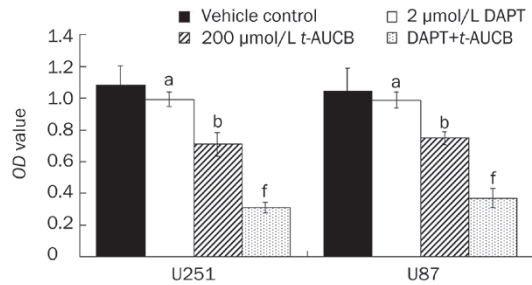


Figure 1. DAPT strengthens *t*-AUCB-induced cell growth suppression. U251 and U87 cells were treated for 48 h with DMSO (vehicle control), 2 $\mu\text{mol/L}$ DAPT only, 200 $\mu\text{mol/L}$ *t*-AUCB, or 200 $\mu\text{mol/L}$ *t*-AUCB with a 4-h pre-treatment of 2 $\mu\text{mol/L}$ DAPT. Cell growth was detected using cell counting kit-8 (CCK-8) and measured by the OD values. The results showed that *t*-AUCB can induce cell growth inhibition, but the pre-treatment of DAPT significantly strengthened the cell growth inhibitory effect induced by *t*-AUCB. DAPT causes no cell growth inhibition. ^a $P > 0.05$, ^b $P < 0.05$ vs vehicle. ^f $P < 0.01$ vs *t*-AUCB.

induced cell growth inhibition ($P < 0.05$). However, with a pre-treatment of DAPT, the cell growth inhibitory effect of *t*-AUCB increased significantly ($P < 0.01$). DAPT alone did not cause cell growth inhibition ($P > 0.05$), which suggests that DAPT plays a role in strengthening the effect of *t*-AUCB-induced cell growth suppression.

t-AUCB induces significant cell apoptosis with pre-treatment of DAPT

We previously revealed that apoptosis cannot be detected even when U251 and U87 cells are treated with 200 $\mu\text{mol/L}$ *t*-AUCB for 72 h because of the apoptosis resistance^[3]. In the present study, however, we detected a significantly strengthened cell growth suppression induced by 200 $\mu\text{mol/L}$ *t*-AUCB with the addition of a pre-treatment of DAPT, indicating that *t*-AUCB may induce apoptosis in the presence of DAPT. To investigate whether *t*-AUCB induces significant cell apoptosis with pre-treatment of DAPT, U251 and U87 cells were treated for 72 h with DMSO (vehicle control), 2 $\mu\text{mol/L}$ DAPT only, 200 $\mu\text{mol/L}$ *t*-AUCB, or 200 $\mu\text{mol/L}$ *t*-AUCB pre-treated with 2 $\mu\text{mol/L}$ DAPT for 4 h. Cell apoptosis was analyzed by flow cytometry using annexin V-FITC conjugates and propidium iodide double staining. The results show that for the vehicle control of U251 or U87 cells, the proportion of Q2 plus Q4 sections (apoptosis) was 3.6% \pm 1.1% or 3.1% \pm 1.4% (Figure 2A and 2E). For the U251 or U87 cells treated with 200 $\mu\text{mol/L}$ *t*-AUCB for 72 h, the proportion of apoptosis was 4.5% \pm 1.8% or 5.1% \pm 1.5% ($P > 0.05$) (Figure 2B and 2F). For the cells treated with 2 $\mu\text{mol/L}$ DAPT for 72 h, the proportion of apoptosis was 6.1% \pm 0.9% or 6.6% \pm 1.7% ($P > 0.05$) (Figure 2C and 2G). For the cells first treated with 2 $\mu\text{mol/L}$ DAPT for 4 h and then with 200 $\mu\text{mol/L}$ *t*-AUCB for 72 h, the proportion of apoptosis was 21.9% \pm 3.6% or 20.8% \pm 2.1% ($P < 0.01$) (Figure 2D and 2H).

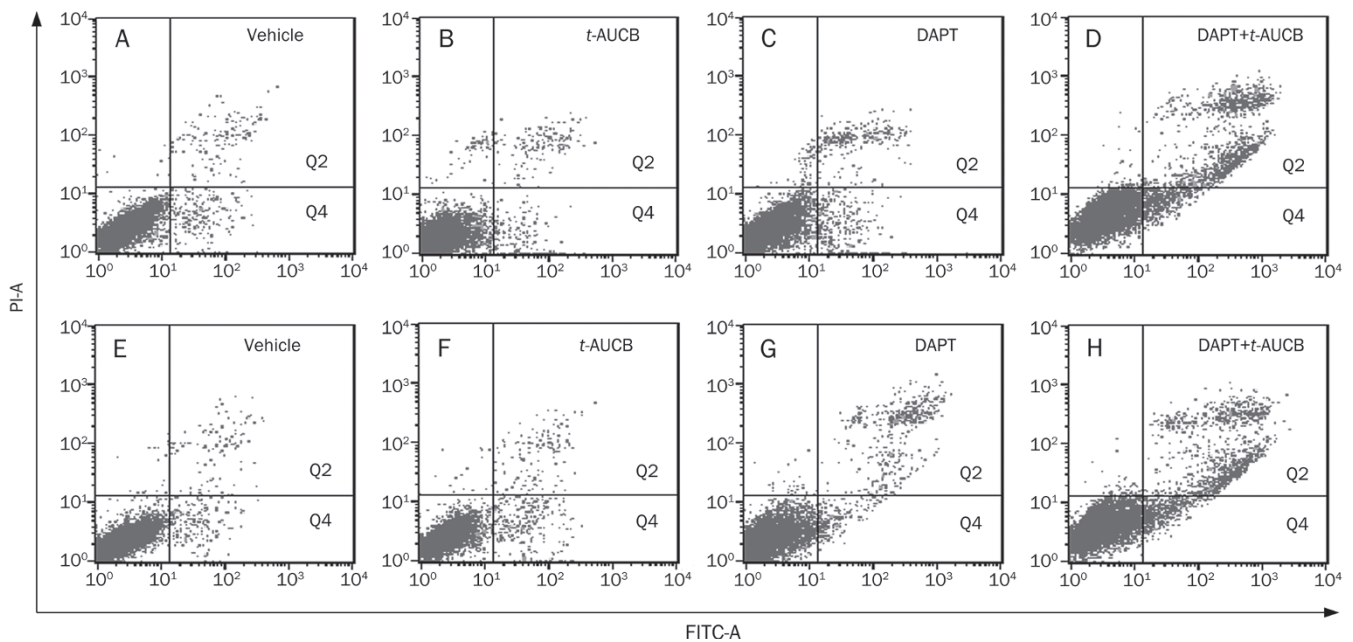


Figure 2. *t*-AUCB induces significant cell apoptosis with the pre-treatment of DAPT. U251 and U87 cells were treated for 72 h with DMSO (vehicle control), 2 $\mu\text{mol/L}$ DAPT, 200 $\mu\text{mol/L}$ *t*-AUCB, or 200 $\mu\text{mol/L}$ *t*-AUCB with a 4-h pre-treatment of 2 $\mu\text{mol/L}$ DAPT. Apoptosis was analyzed with Annexin V-FITC conjugates and PI double staining by flow cytometry. For the vehicle control of U251 (upper panels) or U87 cells (lower panels), the proportion of Q2 plus Q4 sections (apoptosis) was 4.6% \pm 1.1% (A) or 4.1% \pm 1.4% (E). The proportion of apoptosis in 200 $\mu\text{mol/L}$ *t*-AUCB-treated U251 or U87 cells was indicated in each panel.

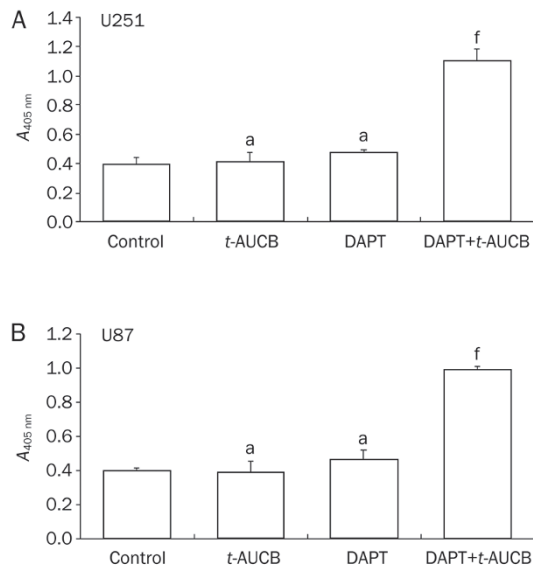


Figure 3. With the pre-treatment of DAPT, *t*-AUCB significantly increased caspase-3 activity. U251 (A) or U87 (B) cells were either untreated, treated only with 200 $\mu\text{mol/L}$ *t*-AUCB for 72 h, treated only with 2 $\mu\text{mol/L}$ DAPT for 72 h, or pre-treated with 2 $\mu\text{mol/L}$ DAPT for 4 h followed by 72 h-treatment of 200 $\mu\text{mol/L}$ *t*-AUCB. Caspase-3 activity was measured using an assay kit. Absorbance read at 405 nm represented the level of caspase-3 activity. The results showed that no significant change in caspase-3 activity was observed in cells only treated with 200 $\mu\text{mol/L}$ *t*-AUCB or 2 $\mu\text{mol/L}$ DAPT for 72 h. In cells with the pre-treatment of DAPT followed by the treatment of *t*-AUCB, the activity of caspase-3 was significantly greater than in those treated with *t*-AUCB only. ^a $P>0.05$ vs Control. ^f $P<0.01$ vs *t*-AUCB.

The caspase-3 activity analysis also showed that cells pre-treated with DAPT before being treated with *t*-AUCB had significantly greater caspase-3 activity compared to those treated with *t*-AUCB only ($P<0.01$) (Figure 3). These data revealed that *t*-AUCB induces significant glioblastoma cell apoptosis with a pre-treatment of DAPT, which indicates that DAPT at low concentrations (without significant cell growth inhibition) can overcome the apoptosis resistance in *t*-AUCB-treated U251 and U87 cells.

DAPT blocks *t*-AUCB-induced activation of the p38 MAPK/MAPKAPK2/Hsp27 pathway and inhibits expression of NICD1

In a recent study, we demonstrated that *t*-AUCB-induced apoptosis resistance in U251 and U87 cells depends on the activation of the p38 MAPK/MAPKAPK2/Hsp27 pathway, which is induced by itself^[3]. In this study, we detected the activation of the p38 MAPK/MAPKAPK2/Hsp27 pathway in cells treated for 48 h with DMSO (vehicle control), 2 $\mu\text{mol/L}$ DAPT only, 200 $\mu\text{mol/L}$ *t*-AUCB only, or 200 $\mu\text{mol/L}$ *t*-AUCB with a 4-h pre-treatment of 2 $\mu\text{mol/L}$ DAPT using Western blots with antibodies against phosphorylated p38 MAPK (Thr180/Tyr182), phosphorylated MAPKAPK2 (Thr334), and phosphorylated Hsp27 (Ser78). GAPDH served as a loading control. The gray value of each immunoblotting band was

measured using ImageJ. The relative gray values of p-p38/p38, p-MAPKAPK2/MAPKAPK2, and p-Hsp27/Hsp27 were calculated and quantified by their phosphorylation levels. Compared with the vehicle control (-), the phosphorylation levels of p38 MAPK, MAPKAPK2, and Hsp27 were significantly greater in cells treated with 200 $\mu\text{mol/L}$ *t*-AUCB ($P<0.01$). In cells treated with DAPT before *t*-AUCB, the phosphorylation levels were very low, with no significant increase ($P>0.05$) (Figure 4). This result indicates that DAPT blocks *t*-AUCB-induced activation of the p38 MAPK/MAPKAPK2/Hsp27 pathway.

Because DAPT was widely used to block Notch signaling by inhibiting the last proteolytic step before the release of NICDs, which is essential for Notch activation, we measured the expression of NICD1 in cells treated for 48 h with DMSO (vehicle control), 2 $\mu\text{mol/L}$ DAPT only, 200 $\mu\text{mol/L}$ *t*-AUCB, or 200 $\mu\text{mol/L}$ *t*-AUCB with 4-h pre-treatment of 2 $\mu\text{mol/L}$ DAPT using Western blotting. Antibodies against NICD1 were used, and GAPDH served as the protein-loading control. The relative gray values were measured using ImageJ and then calculated. The results showed that compared with the vehicle control (-), the DAPT treatment significantly down-regulates NICD1 expression in cells with or without treatment of *t*-AUCB ($P<0.01$) (Figure 5).

Discussion

Glioblastomas (GBMs) are the most common primary malignant brain tumors in adults^[6]. Even with excellent surgery followed by the standard treatment of temozolomide (TMZ) with concurrent external beam radiation as adjuvant therapy, the prognosis of patients with GBMs remains poor^[7-10].

We recently studied the effects of an improved SEH inhibitor, *t*-AUCB, on GBM cells. Our results demonstrated that *t*-AUCB can suppress GBM cell growth, but GBM cells resist *t*-AUCB-induced apoptosis^[2, 3]. The apoptosis resistance was found to depend on the activation of Hsp27 induced by *t*-AUCB itself, which can be overridden with the Hsp27 inhibitor. However, Hsp27 inhibitors are rarely reported in studies associated with anti-gliomas, and thus, their application in *in vivo* studies or clinical trials is limited. Therefore, it is necessary to develop other potential agents that can be widely used and can inhibit the *t*-AUCB-induced activation of Hsp27 or sensitize *t*-AUCB-induced apoptosis.

The γ -secretase inhibitors (GSIs) have been reported to block the generation of a β peptide associated with Alzheimer's disease because of their potential to block the presenilin- γ -secretase complex^[4]. Recently, they were widely used as a tool in anti-cancer studies. An increasing number of reports are revealing that GSIs offer a potential clinical application in cancer therapeutics, including treatment of glioblastomas^[11-16]. A phase I trial of the γ -secretase inhibitor MK-0752 has been performed, and the results show that it is well-tolerated in children with recurrent CNS malignancies. The phase II study was recommended, thus indicating that studies of GSI clinical application are making progress^[17]. A recent study investigated the effects of the Notch pathway blockade by

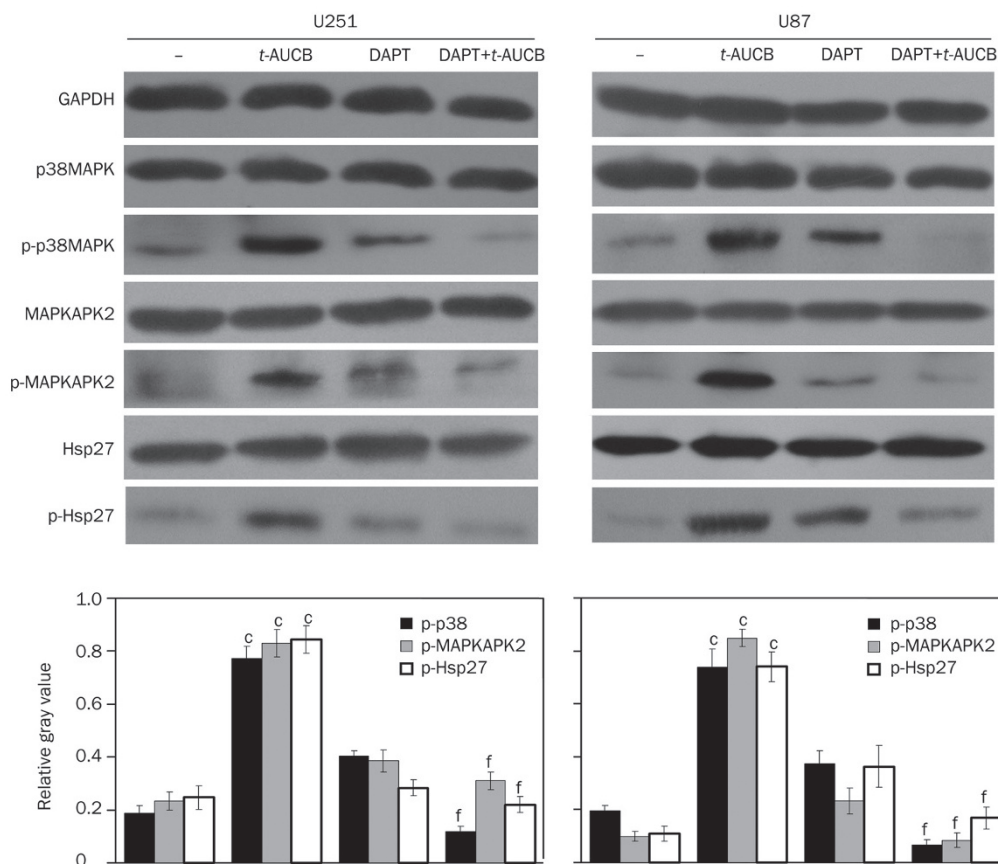


Figure 4. DAPT blocks *t*-AUCB-induced activation of the p38 MAPK/MAPKAPK2/Hsp27 pathway. The activation of p38 MAPK, MAPKAPK2, and Hsp27 was detected by Western blotting using antibodies against phosphorylated p38 MAPK (Thr180/Tyr182), phosphorylated MAPKAPK2 (Thr334), and phosphorylated Hsp27 (Ser78). The total protein levels for each were also measured. GAPDH served as a loading control. The relative gray values of p-p38/p38, p-MAPKAPK2/MAPKAPK2, and p-Hsp27/Hsp27 were calculated with the ImageJ program using their measured gray values and represented the phosphorylation levels of p38 MAPK, MAPKAPK2, and Hsp27. In the vehicle control (-), the phosphorylation levels of p38 MAPK, MAPKAPK2, and Hsp27 were very low. After the 48-h treatment with 200 $\mu\text{mol/L}$ *t*-AUCB, the phosphorylation levels of p38 MAPK, MAPKAPK2, and Hsp27 increased significantly. In cells pre-treated with DAPT before the treatment of *t*-AUCB, the phosphorylation levels were very low, with no significant change compared to the vehicle control, thus indicating that DAPT blocks the *t*-AUCB-induced activation of the p38 MAPK/MAPKAPK2/Hsp27 pathway. ^c $P < 0.01$ vs vehicle control. ^f $P < 0.01$ vs *t*-AUCB.

GSI on GBMs. The authors demonstrated that the blockage of the Notch pathway depletes stem-like cells in GBMs and inhibits tumor growth, which suggests that GSIs may be useful as chemotherapeutic reagents that can target Cancer Stem Cells in malignant gliomas^[18]. Another study on GSIs and GBMs showed that the inhibition of the Notch pathway with GSIs renders the glioma stem cells more sensitive to radiation at clinically relevant doses^[19]. Similarly, the Lin research group described a possibility that a tripeptide GSI (z-Leu-leu-Nle-CHO) called GSI-I could be used at low concentrations to strengthen the radiosensitivity of glioblastoma cells^[5]. Because GSI can sensitize GBM cells to radiation, questions remain regarding its effects on *t*-AUCB-treated GBM cells or whether it can sensitize *t*-AUCB-induced apoptosis.

In the present study, we investigated the effects of the GSI DAPT on *t*-AUCB-treated U251 and U87 glioblastoma cells. First, we detected cell growth and cell apoptosis in cells treated with DAPT only or in those treated with DAPT fol-

lowed by *t*-AUCB. Because DAPT itself can also inhibit cell growth at certain concentrations and to avoid this effect, we applied DAPT at a low concentration of 2 $\mu\text{mol/L}$, which was demonstrated by others^[19-22] and our current study have no significant effects on cell growth inhibition or cell apoptosis induction. Our results showed that with the pre-treatment of DAPT, cell growth inhibition in *t*-AUCB-treated U251 and U87 glioblastoma cells was strengthened significantly. Treatment of DAPT plus *t*-AUCB can induce significant cell apoptosis and promote caspase-3 activity, which is essential in the apoptosis process. DAPT is widely used as a tool to block the Notch signaling pathway in studies of cancer therapy and can hence override chemoresistance by inhibiting the expression of Notch1^[23]. Thus, we herein detected the levels of Notch1 intracellular domain (NICD1) and the active region of the Notch1 receptor of cells under different experimental treatments by western blot.

We found that DAPT significantly downregulated the level

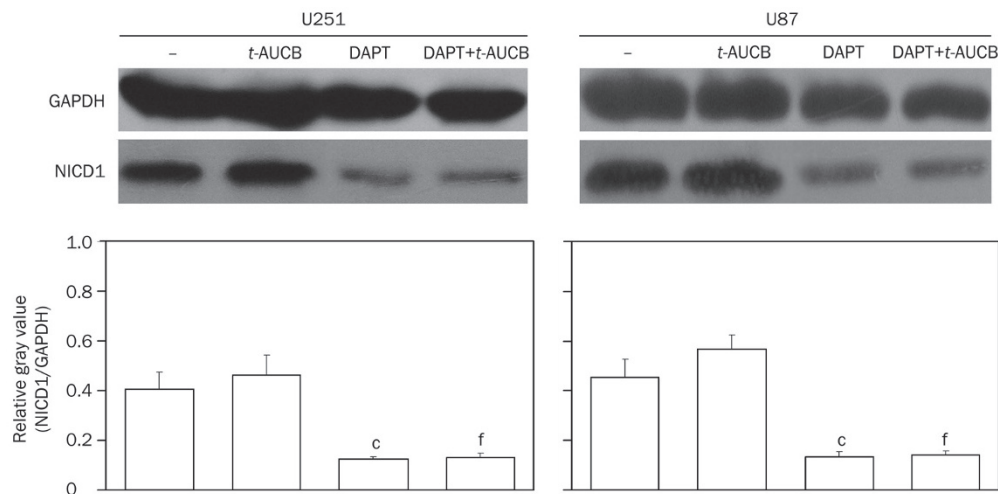


Figure 5. DAPT downregulates NICD1 expression in cells with or without *t*-AUCB. The expression level of NICD1 was detected by Western blotting using antibodies against the Notch1 intracellular region. GAPDH served as a loading control. The relative gray values of NICD1/GAPDH were calculated using gray values measured by ImageJ and represented as the expression level of NICD1. In the vehicle control (-) and cells with 48-h treatment of 200 μ mol/L *t*-AUCB, NICD1 was highly expressed. In cells treated with 2 μ mol/L DAPT only for 48 h or pre-treated with 2 μ mol/L DAPT for 4 h followed by 48-h treatment of 200 μ mol/L *t*-AUCB, the expression level of NICD1 significantly decreased. ^c $P < 0.01$ vs control. ^f $P < 0.01$ vs *t*-AUCB.

of NICD1 in GBM cells no matter whether they were treated with *t*-AUCB or not. We previously demonstrated that the apoptosis resistance in *t*-AUCB-treated GBM cells depends on the activation of Hsp27^[3]. Therefore, we suggest that DAPT may affect the activation of Hsp27. Our results from the Western blot analysis showed that DAPT can block the *t*-AUCB-induced activation of the p38 MAPK/MAPKAPK2/Hsp27 pathway, thus indicating that DAPT is a potential agent that can inhibit the *t*-AUCB-induced activation of Hsp27 and increase *t*-AUCB-induced apoptosis in glioblastoma cells. Although a study researching the formation of actin stress fibers^[24] reported that a peptide, GSI (Z-Leu-Lyu-Nle-CHO), can completely block the activation of the p38 MAPK/MAPKAPK2/Hsp27 pathway, almost no previous studies report that GSIs can be used to overcome chemoresistance in tumors by blocking the activation of the p38 MAPK/MAPKAPK2/Hsp27 pathway. In the present study, we demonstrated that the GSI DAPT blocks the *t*-AUCB-induced activation of the p38 MAPK/MAPKAPK2/Hsp27 pathway in human GBM cells. We also showed that *t*-AUCB, when combined with DAPT, is effective for inducing U251 and U87 cell apoptosis.

In conclusion, our results demonstrated that the GSI DAPT can target the p38 MAPK/MAPKAPK2/Hsp27 pathway to overcome *t*-AUCB-induced apoptosis resistance in human glioblastoma U251 and U87 cells. This suggests that targeting of the p38 MAPK/MAPKAPK2/Hsp27 pathway with a γ -secretase inhibitor may be a novel approach for overcoming chemoresistance in cancer therapy. The combination of *t*-AUCB and the GSI DAPT may be a potential strategy for the treatment of GBM.

Acknowledgements

We thank Prof Bruce D HAMMOCK for providing the sEH

inhibitor *t*-AUCB. This study was supported by the National Natural Science Foundation of China (No 81070974 and No 81301905).

Author contribution

Jun-yang LI and Han-dong WANG designed the research; Jun-yang LI and Ru-jun LI performed the research; Jun-yang LI analyzed the data; Jun-yang LI wrote the paper; and Han-dong WANG revised the paper.

References

- Liu JY, Tsai HJ, Hwang SH, Jones PD, Morisseau C, Hammock BD. Pharmacokinetic optimization of four soluble epoxide hydrolase inhibitors for use in a murine model of inflammation. *Br J Pharmacol* 2009; 156: 284–96.
- Li J, Liu H, Xing B, Yu Y, Wang H, Chen G, *et al.* *t*-AUCB, an improved sEH inhibitor, suppresses human glioblastoma cell growth by activating NF- κ B-p65. *J Neurooncol* 2012; 108: 385–93.
- Li J, Hu W, Lan Q. The apoptosis-resistance in *t*-AUCB-treated glioblastoma cells depends on activation of Hsp27. *J Neurooncol* 2012; 110: 187–94.
- Shih le M, Wang TL. Notch signaling, gamma-secretase inhibitors, and cancer therapy. *Cancer Res* 2007; 67: 1879–82.
- Lin J, Zhang XM, Yang JC, Ye YB, Luo SQ. Gamma-secretase inhibitor-I enhances radiosensitivity of glioblastoma cell lines by depleting CD133+ tumor cells. *Arch Med Res* 2010; 41: 519–29.
- Stupp R, Mason WP, van den Bent MJ, Weller M, Fisher B, Taphoorn MJ, *et al.* Radiotherapy plus concomitant and adjuvant temozolomide for glioblastoma. *N Engl J Med* 2005; 352: 987–96.
- Karayan-Tapon L, Quillien V, Guilhot J, Wager M, Fromont G, Saikali S, *et al.* Prognostic value of O6-methylguanine-DNA methyltransferase status in glioblastoma patients, assessed by five different methods. *J Neurooncol* 2010; 97: 311–22.
- Minniti G, Salvati M, Arcella A, Buttarelli F, D'Elia A, Lanzetta G, *et al.* Correlation between O6-methylguanine-DNA methyltransferase and

- survival in elderly patients with glioblastoma treated with radiotherapy plus concomitant and adjuvant temozolomide. *J Neurooncol* 2011; 102: 311–6.
- 9 Fan J, Ou YW, Wu CY, Yu CJ, Song YM, Zhan QM. Migfilin sensitizes cisplatin-induced apoptosis in human glioma cells *in vitro*. *Acta Pharmacol Sin* 2012; 33: 1301–10.
 - 10 Li JY, Huang JY, Li M, Zhang H, Xing B, Chen G, et al. Anisomycin induces glioma cell death via down-regulation of PP2A catalytic subunit *in vitro*. *Acta Pharmacol Sin* 2012; 33: 935–40.
 - 11 Nefedova Y, Sullivan DM, Bolick SC, Dalton WS, Gabrilovich DI. Inhibition of Notch signaling induces apoptosis of myeloma cells and enhances sensitivity to chemotherapy. *Blood* 2008; 111: 2220–9.
 - 12 Curry CL, Reed LL, Golde TE, Miele L, Nickoloff BJ, Foreman KE. Gamma secretase inhibitor blocks Notch activation and induces apoptosis in Kaposi's sarcoma tumor cells. *Oncogene* 2005; 24: 6333–44.
 - 13 Meng RD, Shelton CC, Li YM, Qin LX, Notterman D, Paty PB, et al. Gamma-secretase inhibitors abrogate oxaliplatin-induced activation of the Notch-1 signaling pathway in colon cancer cells resulting in enhanced chemosensitivity. *Cancer Res* 2009; 69: 573–82.
 - 14 Weng AP, Nam Y, Wolfe MS, Pear WS, Griffin JD, Blacklow SC, et al. Growth suppression of pre-T acute lymphoblastic leukemia cells by inhibition of notch signaling. *Mol Cell Biol* 2003; 23: 655–64.
 - 15 Purow BW, Haque RM, Noel MW, Su Q, Burdick MJ, Lee J, et al. Expression of Notch-1 and its ligands, Delta-like-1 and Jagged-1, is critical for glioma cell survival and proliferation. *Cancer Res* 2005; 65: 2353–63.
 - 16 Kanamori M, Kawaguchi T, Nigro JM, Feuerstein BG, Berger MS, Miele L, et al. Contribution of Notch signaling activation to human glioblastoma multiforme. *J Neurosurg* 2007; 106: 417–27.
 - 17 Fouladi M, Stewart CF, Olson J, Wagner LM, Onar-Thomas A, Kocak M, et al. Phase I trial of MK-0752 in children with refractory CNS malignancies: a pediatric brain tumor consortium study. *J Clin Oncol* 2011; 29: 3529–34.
 - 18 Fan X, Khaki L, Zhu TS, Soules ME, Talsma CE, Gul N, et al. NOTCH pathway blockade depletes CD133-positive glioblastoma cells and inhibits growth of tumor neurospheres and xenografts. *Stem Cells* 2010; 28: 5–16.
 - 19 Wang J, Wakeman TP, Lathia JD, Hjelmeland AB, Wang XF, White RR, et al. Notch promotes radioresistance of glioma stem cells. *Stem Cells* 2010; 28: 17–28.
 - 20 Zhou JX, Han JB, Chen SM, Xu Y, Kong YG, Xiao BK, et al. Gamma-secretase inhibition combined with cisplatin enhances apoptosis of nasopharyngeal carcinoma cells. *Exp Ther Med* 2012; 3: 357–61.
 - 21 Wang Z, Li Y, Banerjee S, Kong D, Ahmad A, Nogueira V, et al. Down-regulation of Notch-1 and Jagged-1 inhibits prostate cancer cell growth, migration and invasion, and induces apoptosis via inactivation of Akt, mTOR, and NF-kappaB signaling pathways. *J Cell Biochem* 2010; 109: 726–36.
 - 22 Irusta G, Pazos MC, Abramovich D, De Zuniga I, Parborell F, Tesone M. Effects of an inhibitor of the gamma-secretase complex on proliferation and apoptotic parameters in a FOXL2-mutated granulosa tumor cell line (KGN). *Biol Reprod* 2013; 89: 9.
 - 23 Liu YP, Yang CJ, Huang MS, Yeh CT, Wu AT, Lee YC, et al. Cisplatin selects for multidrug-resistant CD133+ cells in lung adenocarcinoma by activating Notch signaling. *Cancer Res* 2013; 73: 406–16.
 - 24 Song C, Perides G, Wang D, Liu YF. Beta-amyloid peptide induces formation of actin stress fibers through p38 mitogen-activated protein kinase. *J Neurochem* 2002; 83: 828–36.